Available online at www.sciencedirect.com

ScienceDirect

Current Opinion in
Colloid & Interface Science

Molecular and colloidal self-assembly at the oil–water interface

Guangle Li[1] and Yi Y. Zuo[1,2]

Abstract

Self-assembly is a versatile bottom-up approach for fabricating novel supramolecular materials with well-defined nano- or micro-structures associated with functionalities. The oil-water interface provides an ideal venue for molecular and colloidal self-assembly. This paper gives an overview of various self-assembled materials, including nanoparticles, polymers, proteins, and lipids, at the oil-water interface. Focus has been given to fundamental principles and strategies for engineering the self-assembly process, such as control of pH, ionic strength and use of external fields, to achieve complex soft materials with desired functionalities, such as nanoparticle surfactants, structured liquids, and proteinosomes. It has been shown that self-assembly at the oil-water interface holds great promise for developing well-structured complex materials useful for many research and industrial applications.

Addresses

[1] Department of Mechanical Engineering, University of Hawaii at Manoa, Honolulu, HI 96822, United States
[2] Department of Pediatrics, John A. Burns School of Medicine, University of Hawaii, Honolulu, HI 96826, United States

Corresponding author: Zuo, Yi Y. (yzuo@hawaii.edu)

Current Opinion in Colloid & Interface Science 2022, **62**:101639

This review comes from a themed issue on **Self Assembly**

Edited by **Junbai Li**

For a complete overview see the Issue and the Editorial

https://doi.org/10.1016/j.cocis.2022.101639

Keywords

Self-assembly, Oil-water interface, Interfacial tension, Nanoparticle surfactant, Phospholipid.

Introduction

Self-assembly provides a powerful bottom-up approach for fabricating stable structurally-defined supramolecular materials associated with functionalities. A variety of molecules, *e.g.*, lipids, peptides, proteins, and polymers, have been studied as the building blocks for engineering novel synthetic materials [1–3]. With the rise of nanotechnology, the building block of self-assembly has been expanded from molecules to colloidal particles, including engineered nanomaterials, which can be modified to self-assemble into complex and functional structures [4]. These self-assembled materials have demonstrated a great potential in many research and industrial fields, including catalysis, sensing, biotechnology, and electronics [5–8].

In general, molecular and colloidal self-assembly is a spontaneous thermodynamic process that is mediated by weak, noncovalent interactions such as hydrogen bonds, van der Waals forces, electrostatic, and hydrophobic interactions [9]. Early research was mostly focused on molecular self-assembly in the bulk phase. More recently, interfacial self-assembly has attracted extensive attention due to its unique nature for constructing functional hierarchical superstructures, *e.g.*, 2D films and 3D capsules, at two-phase interfaces [10,11].

Molecular and colloidal self-assembly at the oil-water interface has many important applications in complex fluids, synthetic biology, food and nutrition, environmental remediation, enhanced oil recovery, and enhanced organic synthesis [12–16]. The oil-water interface provides an ideal platform for engineering self-assemblies with novel mechanical and functional properties [17]. In particular, the oil-water interface is mostly encountered in emulsions, which are droplets of one liquid phase dispersed at the nanoscale or microscale in a second immiscible liquid. From a thermodynamic perspective, emulsions are energetically unstable and always subject to droplet coalescence, or inevitable phase separation. Self-assembly of amphiphilic molecules and/or particles at the interface makes emulsions thermodynamically or kinetically stable. Among these emulsions, microemulsions have been increasingly utilized for encapsulating bioactive components in the food and pharmaceutical industries [18]. A typical microemulsion is a clear, thermodynamically stable isotropic dispersion with surfactants self-assembled at the oil-water interface [19]. The droplet size distribution of microemulsions generally ranges from about 10 nm to 300 nm [20]. Besides their tremendous industrial applications, microemulsions can act as soft templates for fabricating highly-ordered arrays, closely-packed coatings, and superstructures with hierarchical patterns [21–24]. To date, self-assembly at the oil-water interface has been used to create various supramolecular structures, such as

colloidosomes, proteinosomes, Janus structures, and non-equilibrium structured liquids [17,25–27].

This review will be focused on recent development of molecular and colloidal self-assemblies at the oil-water interface. As shown in Figure 1, our discussion will be limited to the self-assembly of particles, polymers, proteins, and lipids. Among these materials, polymers, proteins, and phospholipids are self-assembled at the oil-water interface spontaneously because of their amphiphilicity. Microparticles, generally referring to particles larger than 1 μm in diameter, usually adsorb to the oil-water interface irreversibly by significantly reducing the system energy. However, nanoparticles, generally referring to particles less than 1 μm or often to those less than 100 nm, usually only adsorb reversibly to the oil-water interface since they are subject to substantially more thermal fluctuation than microparticles. We will discuss the common methods used to engineer various molecular and colloidal self-assembly processes, including the control of pH and ionic strength. Novel applications of the self-assembled materials will also be discussed.

Self-assembly of particles at the oil-water interface

Self-assembly of colloidal particles at fluid interfaces was first reported by Pickering and Ramsden about a century ago, and the emulsions stabilized by colloidal particles are now known as "Pickering emulsions" [28,29]. Pickering emulsions can be either oil-in-water or water-in-oil types, depending on the wettability of the particles, which can be described by the contact angle at the oil-water interface (Figure 2a) [11]. Pickering emulsions can be more stable than the traditional emulsions stabilized by surfactants, due to the significant reduction in interfacial energy by solid particles that bind to the interface. Pickering emulsions have been applied to fabricate colloidosomes whose shells are composed of densely packed colloidal particles [25]. Colloidal particles are initially self-assembled at the oil-water interface, followed by shell reinforcement *via*

Figure 1

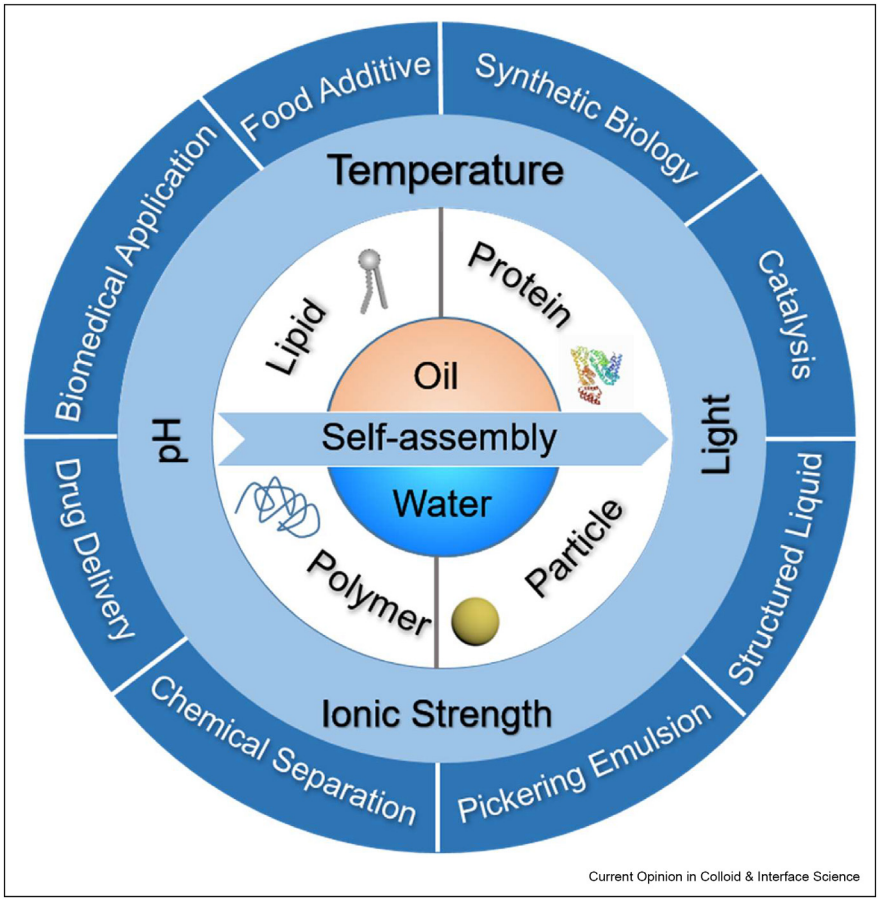

Self-assembly of four common materials, *i.e.*, particles, polymers, proteins, and lipids, at the oil-water interface, the external stimuli that can be used to control the self-assembly process, and representative applications of the self-assembled materials.

Figure 2

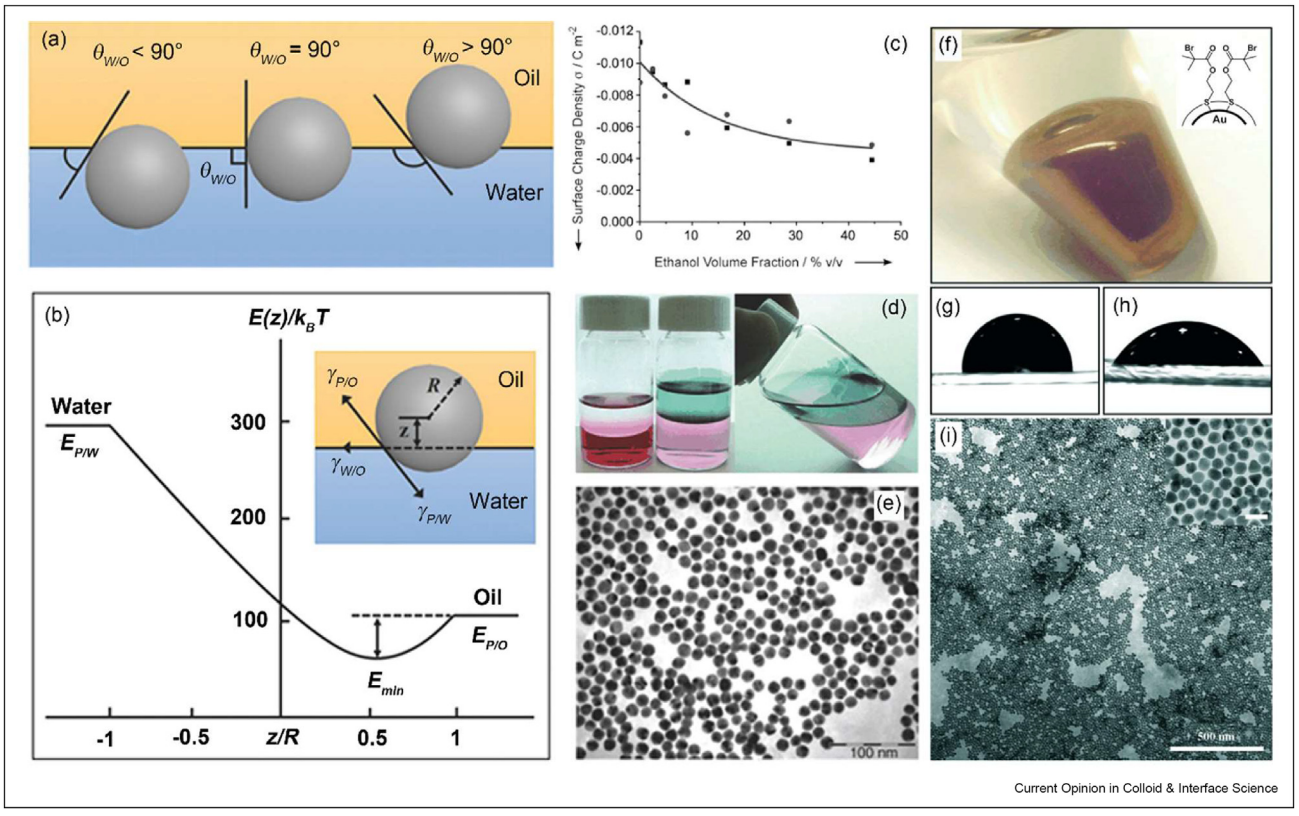

Self-assembly of colloidal particles at the oil-water interface. (**a**) Schematic representation of the position of a spherical particle at the oil-water interface for a contact angle less than 90° (left), equal to 90° (center), and larger than 90° (right). (b) Surface free energy of particle adsorption at the oil-water interface. Reproduced with permission [11]. Copyright 2018, Wiley-VCH. (**c**) Decrease of the surface charge density of AuNPs upon adding ethanol to the aqueous sol consisting of AuNPs. (**d**) Left: an aqueous AuNPs sol (pink) covered with heptane (colorless); center and right: after addition of 4 mL ethanol to the sol, an AuNPs layer (blue) is formed at the heptane–water interface and extends up to the heptane–glass interface. (**e**) TEM image of a layer of AuNPs with a maximum coverage (65%) collected from the heptane–water interface. Reproduced with permission [36]. Copyright 2004, Wiley-VCH. (**f**) Photograph of the self-assembled AuNPs modified with 2,2′-dithiobis [1-(2-bromo-2-methylpropionyloxy) ethane] (DTBE) (Au@DTBE) at the toluene–water interface. This tube has been tilted such that the colored area corresponds to the toluene–water interface. Owing to the reflectance from the sides, only the blue-purple area represents a transmission image. The inset shows the schematic illustration of the structures of Au@DTBE. (**g**, **h**) Contact angles of a 5-μL water droplet, covered with toluene, resting on the surface of a thin film of 12-nm Au@DTBE NPs, transferred from the toluene–water interface on a glass slide (**g**) and on the surface of a thin film of 12-nm AuNPs cast on a glass side (**h**). (**i**) TEM image of a monolayer of 12-nm Au@DTBE NPs, formed at the toluene–water interface. Reproduced with permission [37] Copyright 2004, Wiley-VCH.

addition of polyelectrolyte, gel trapping, covalent cross-linking, or sintering [30]. Various particles, *e.g.*, polymer latex and metal oxide, with different shapes, have been studied thoroughly for fabricating colloidosomes [31,32]. Colloidosomes have shown potential applications in microencapsulation for the controlled release of active ingredients.

Colloidal self-assembly is driven by the reduction of interfacial energy upon particle adsorption to the oil-water interface (Figure 2b) [11,33]. Adsorption of particles with a radius r at the oil-water interface leads to a decrease in the system energy from E_0, *i.e.*, the energy of the oil-water interface, to E_{min}, *i.e.*, the minimum energy with the interface covered with a monolayer of particles, yielding an energy difference ΔE:

$$\Delta E = E_{min} - E_0 = -\frac{\pi r^2}{\gamma_{W/O}}\left[\gamma_{W/O} - \left|\gamma_{P/W} - \gamma_{P/O}\right|\right]^2 \quad (1)$$

where, $\gamma_{W/O}$, $\gamma_{P/W}$, and $\gamma_{P/O}$, are the interfacial energies between oil and water, particle and water, and particle and oil, respectively. Using the Young–Dupré equation [34], Eq. (1) can be rewritten into:

$$\Delta E = -\pi r^2 \gamma_{W/O}\left(1 - \left|cos\,\theta_{W/O}\right|\right)^2 \quad (2)$$

where, $\theta_{W/O}$ is the contact angle of particles at the oil-water interface, which reflects the preferential wetting by either the oil phase or the aqueous phase. Thus, it can be seen

that at certain interfacial tension, the decrease of the total free energy ΔE is dominated by the size (r) and wettability ($\theta_{W/O}$) of the particle, respectively. Generally speaking, ΔE must be negative for the colloidal self-assembly to be thermodynamically favored.

Eq. (2) highlights a key difference between microparticles (MPs) and nanoparticles (NPs) with the latter being much less stably adsorbed to the oil-water interface [28]. For MPs, the energy decrease (ΔE) exceeds the thermal energy (k_BT) by several orders of magnitude (up to 10^6 k_BT), which leads to an almost irreversible adsorption of MPs to the interface. However, for NPs, especially those smaller than 10 nm, the magnitude of ΔE is comparable to the thermal fluctuation energy k_BT, thus making NPs easily desorb from the interface. Consequently, self-assembly of NPs at the oil-water interface is mostly dynamic, with NPs adsorbing to and desorbing from the interface simultaneously. For this reason, most traditional Pickering emulsions were stabilized by MPs [29]. The particle size-dependent stability has been demonstrated by Lin et al., who studied the interfacial entrapment of hydrophobic cadmium selenide (CdSe) NPs of different sizes at the toluene–water interface [35]. They found that CdSe NPs less than 1.6 nm did not stabilize the droplet, whereas those with a diameter of 2.8 nm did. When 4.6-nm NPs were added to the toluene phase, they were found to spontaneously displace the 2.8-nm NPs and resulted in a phase separation at the interface.

Besides their size, the contact angle ($\theta_{W/O}$) of particles at the oil-water interface also plays a significant role in determining how the particles partition at the interface. As shown in Figure 2a, when a particle is either hydrophilic or hydrophobic, it has a contact angle either smaller (left) or larger than 90° (right) at the oil-water interface, and the particle tends to be suspended more in the water or in the oil phase. When its contact angle is around 90° (center), the particle prefers to reside at the interface. It can be also predicted by Eq. (2): when $\theta_{W/O}$ is close to 90°, the ΔE reaches a negative maximum, indicating favorable particle adsorption.

Recently, various methods have been developed to enhance interfacial entrapment and self-assembly of NPs at the oil-water interface [36–39]. Hydrophilic NPs were found to be assembled at the interface by simply heating, or adding a solvent miscible with both water and oil, such as acetone or ethanol [36,38]. For example, Reincke et al. studied the assembly of citrate-stabilized gold NPs (AuNPs) at the heptane–water interface with the assistance of ethanol [36]. It was found that the addition of ethanol to the gold aqueous sol particles gradually decreased the surface charge of negatively charged AuNPs (Figure 2c), likely due to the competitive adsorption of ethanol molecules, which displaced citrate anions from the gold surface. In the presence of ethanol, the charged AuNPs had a contact angle close to 90°, leading to a reduction in the interfacial energy and therefore adsorption of AuNPs at the heptane–water interface. A blue layer with a metallic aspect was observed at the interface upon the addition of ethanol to the gold sol (Figure 2d). By analyzing the Langmuir–Blodgett transferred film, the AuNPs coverage of the oil-water interface was determined at around 65% for 16-nm particles, with voids of a typical size equivalent to 1–10 NPs (Figure 2e). The interparticle distance, due to the residual electrostatic repulsions between NPs, was found to be 1–4 nm.

The self-assembly of NPs at the oil-water interface can be also enhanced by modifying the particle surfaces [37,39]. Duan et al. modified 12-nm hydrophilic AuNPs with 2,2′-dithiobis [1-(2-bromo-2-methylpropionyloxy) ethane] (Au@DTBE) by means of ligand exchange [37]. They found that the addition of toluene to the aqueous dispersions of Au@DTBE NPs led to spontaneous transfer onto the toluene–water interface and subsequent self-assembly into a closely-packed thin film (Figure 2f). The Au@DTBE had a 90° contact angle at the toluene–water interface because of the terminal 2-bromopropionate group at the NP surfaces, whereas the contact angle of citrate-stabilized AuNPs was about 60° (Figure 2g *vs.* 2h). The interfacial energy decrease due to the 90° contact angle was the driving force for Au@DTBE NPs to partition into the oil-water interface and to self-assemble into a thin film. However, large voids existed in the closely-packed Au@DTBE NP film (Figure 2i). Formation of these voids was attributed to competitive electrostatic repulsions against long-range van der Waals attractions. Highly ordered NPs with homogeneous microscopic features at the oil-water interface can be obtained by the addition of ethanol and coating of NPs with long-chain alkanethiols, which decreases the electrostatic repulsive forces and increases the van der Waals forces [40].

A latest trend in the development of NP self-assembly at the oil-water interface is the so-called "NP surfactants" [11,17,41,42]. Interactions between NPs and oligomeric/polymeric ligands at the oil-water interface can be used as a versatile technique for promoting NP self-assembly at the interface, increasing interfacial activity, and constructing reconfigurable complex soft materials [17,43]. Because NPs and polymeric ligands have complementary functionalities, they exclusively interact at the interface to promote irreversible NP adsorption, analogous to the behavior of surfactants. When the oil-water interface is deformed, *e.g.*, with an external electric field, the additional surface area generated by the droplet deformation promotes adsorption of more NPs than those allowed to the surface under the equilibrium condition. Hence, when the external field is removed, the excessive NPs at the interface get congested and lose mobility, a

phenomenon known as "interfacial jamming" [11,44]. The jammed NP surfactant layer at the droplet surface prevents droplet relaxation to its lowest energy, *e.g.*, a spherical shape, thus maintaining a kinetically nonequilibrium droplet that has combined characteristics of a fluid and the structural stability of a solid, known as "structured liquids" [17].

Various parameters can be tuned to control the interfacial assembly and packing of the NP surfactants, such as pH, ionic strength of the aqueous phase, concentrations of NPs and polymer ligands, NP size and the molecular weight of polymers [45–47]. Huang et al. systematically studied the effects of pH on the formation of NP surfactants at the toluene–water interface containing carboxylated polystyrene (PS–COOH) NPs in the water phase and amine-terminated polydimethylsiloxane (PDMS-NH_2) in the oil phase (Figure 3a) [45]. At higher pH (>5.0), both ammonium and carboxylate are ionized (PDMS-NH_3^+ and PS-COO^-) and the electrostatic interactions between NPs and polymeric ligands are so significant that facilitate the interfacial formation of NP surfactants. Figure 3b and c show that for pH > 6.0, the interfacial tension is around 22–24 mN/m and the NP surfactants exhibit a wrinkling behavior upon decreasing volume of the droplet, which demonstrates a solid-like structure. The water droplet could be trapped in the ellipsoidal shape after removing the external electric field due to the strong interactions between anionic carboxylates on ionized PS-COOH NPs and the protonated amine terminus of PDMS-NH_2 (Figure 3d). When pH falls near or below the pK_a value of carboxylate (~5.0), the interfacial tension rapidly decreases (Figure 3b and c), and the interactions maintaining the NP surfactants become relatively weak, thus resulting in the ejection of NP surfactants from the interface when decreasing the interfacial area. Consequently, the ellipsoidal droplet relaxes to its equilibrium spherical shape (Figure 3d).

In addition to electrostatic interactions, NP surfactants can be produced by other molecular interactions at the oil-water interface, *e.g.*, host-guest and charge transfer interactions, which allows for multiple stimuli-responsiveness [48,49]. Sun et al. described a photo-responsive structured liquid based on the self-assembly of α-cyclodextrin (α-CD) functionalized 10-nm AuNPs dispersed in water and azobenzene-terminated poly-L-lactide (Azo-PLLA) dissolved in toluene (Figure 3e) [49]. When these two phases contact each other, the interfacial tension rapidly decreases to ~15 mN/m, whereas the pure toluene–water interface has an interfacial tension of 35 mN/m (Figure 3f). TEM images show that a closely-packed AuNPs layer is formed at the toluene–water interface (Figure 3g). The structured droplet relaxes under UV irradiation due to the isomerization of Azo from *trans* to *cis* configurations, resulting in a size mismatch with α-CD and the subsequent break of host-guest interactions (Figure 3h).

Self-assembly of polymers at the oil-water interface

Synthetic amphiphilic oligomers or block copolymers can spontaneously self-assemble at the oil-water interface to form stable and robust nanoscale membranes [50,51]. Self-assembly and conformation of oligomers at the oil-water interface depend on the solvating effects of the oil phase, electrostatic and hydrogen-bonding interactions between the charged headgroups and ionic species in the aqueous phase [51,52]. The self-assembly of oligomers at the air–water surface can be different from that at the oil-water interface because of the absence of the solvating effects of the oil phase. However, new hydrogen bonding between hydrophobic chains and water emerges to stabilize the dilute surface, and this unfavorable interaction must be shielded before the formation of tail–tail interaction upon compression [53].

In addition to amphiphilic polymers, a variety of polymers can co-assemble at the oil-water interface *via* electrostatic interactions and/or molecular recognition between oil-soluble and water-soluble polymers [54,55]. Polymer-based emulsions have been widely studied for encapsulation and delivery of active ingredients such as food additives, drugs, enzymes, as well as microcompartments in protocell research [56]. The flexibility of polymers for conformational changes provides them significant advantages over solid particles used in conventional Pickering emulsions. Unlike colloidal particles, polymers generally have high degrees of entanglement and interpenetration at the interface. Polymeric self-assemblies have the potential to serve as selective membranes for chemical separation and microcompartments in biomimetics [57,58].

Polymer adsorption at the oil-water interface is a complex process in which the hydrophobic backbones of the polymeric macromolecules can coil and bend into a variety of conformations while the hydrophilic functional groups can vary greatly depending on the aqueous phase composition. As shown in Figure 4a, polymer microgels in the bulk phase generally have a core-corona structure with a larger polymer density in the core since the crosslink density often decreases from the center to the periphery [59–61]. Upon adsorption to an oil-water interface, the microgel deforms to increase its contact area. Fractions of the polymer network are stretched and compressed to spread to the interface while other fractions remain in the bulk phase. Intrinsic properties of polymers, such as their charge and length, properties of the aqueous phase, such as its pH and ionic strength, and the oil phase, all have great effects on polymer adsorption at the interface [51,60,62]. Beaman et al.

Figure 3

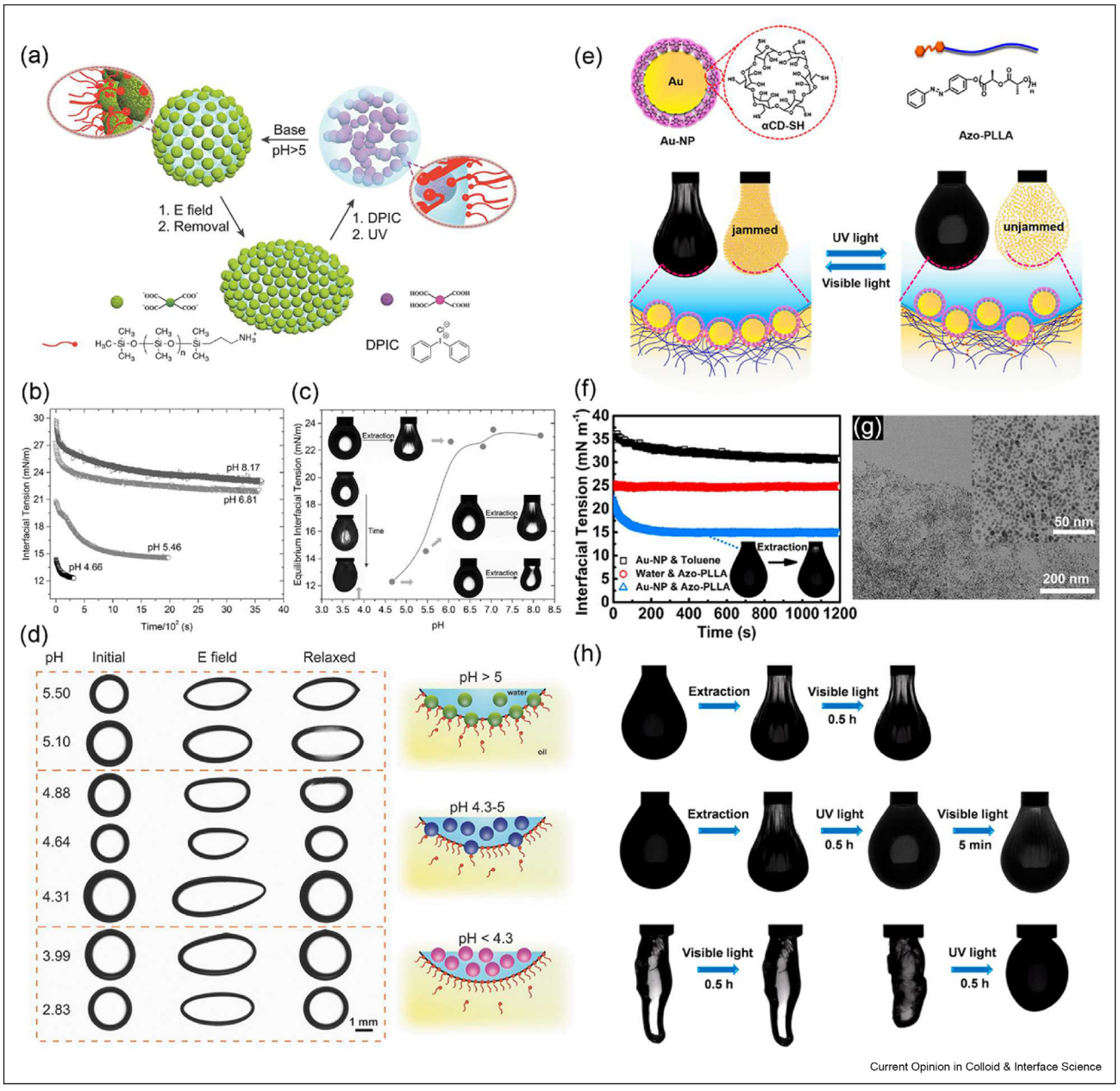

Nanoparticle surfactants with pH responsiveness constructed by electrostatic interaction at the oil-water interface. (**a**) Schematic representation of the reversible pH-responsive liquid drop between equilibrium and nonequilibrium states through jamming and unjamming processes. (**b**, **c**) pH-dependent assembly of NP surfactants at the toluene–water interface. (**d**) Structuring and restructuring liquids through pH-controlled jamming and unjamming of NP surfactants. Reproduced with permission [45]. Copyright 2016, Wiley-VCH. (**e**) Chemical structures of the designed AuNPs and Azo-PLLA, and schematic representation of the photoresponsive NP surfactants at the oil-water interface from the jammed to the unjammed state. (**f**) Time evolution of interfacial tension of NP surfactants obtained by molecular recognition between AuNPs and Azo-PLLA. (**g**) TEM image of a thin film of AuNPs transferred from the interface. (**h**) Morphology evolution of the pendant drop with jammed NP surfactants at the interface under visible light or UV irradiation. Reproduced with permission [49]. Copyright 2020, American Chemical Society.

studied the effect of molecular weight on the assembly of a typical polyelectrolyte, poly (acrylic acid) (PAA), at the chloroform–water interface [63]. As shown in Figure 4b, the adsorption kinetics was highly dependent on the molecular weight of the polymer. While the 1.8 kDa and 450 kD PAA took less than 20 min to reach equilibrium, the 1250 kD PAA took more than 7 h to reach equilibrium, due to slower diffusion of the larger polymer to the interface. Using vibrational sum frequency spectroscopy, it was found that the adsorption

Figure 4

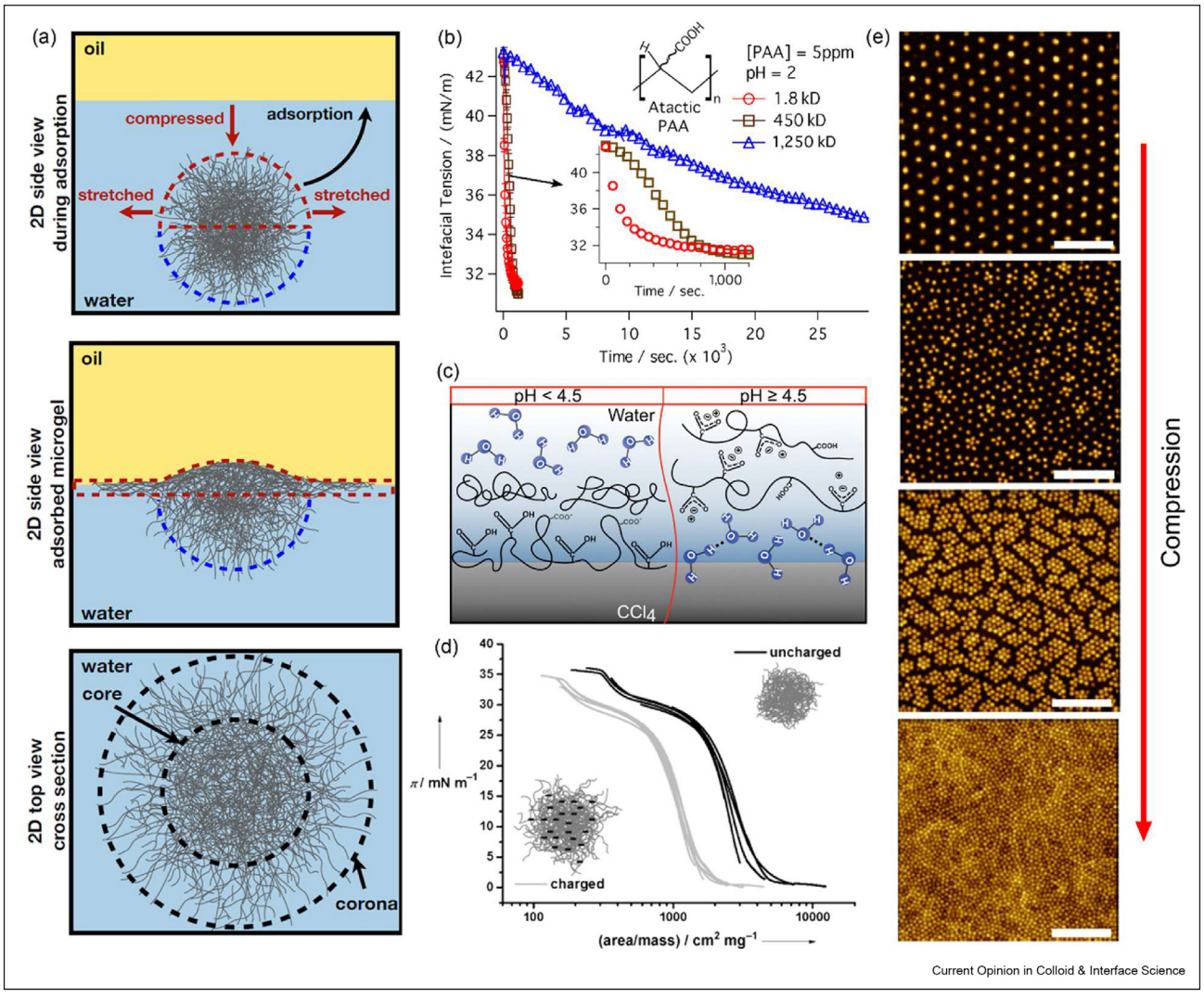

Self-assembly of polymers at the oil-water interface. (**a**) Schematic representation of the conformation of a pNIPAM microgel with inhomogeneous cross-linker distribution at the oil-water interface. Upper: side view during adsorption, middle: side view after adsorption, bottom: 2D top view of a cross-section along the interfacial plane. Reproduced with permission [61]. Copyright 2021, Royal Society of Chemistry. (**b**) Interfacial tension change of the chloroform–water interface upon the introduction of PAA with three different molecular weights, 1.8, 450, 1250 kDa in the aqueous phase. Reproduced with permission [63]. Copyright 2012, National Academy of Science. (**c**) Schematic representation of PAA at the chloroform–water interface for two pH regimes. At low pH (<4.5), polymer adsorbs strongly to the interface with highly oriented carbonyl and CH groups. At high pH (≥4.5), there is a deficit of polymer from the interface, which leaves water molecules close to their normal neat interfacial structure. Reproduced with permission [64]. Copyright 2011, American Chemical Society. (**d**) Compression isotherms of p (NIPAM-co-MAA) microgels in the charged and uncharged states at the decane–water interface. Reproduced with permission [65]. Copyright 2014, Wiley-VCH. (**e**) AFM images of pNIPAM microgels deposited at 20 °C from the decane–water interface at increasing surface pressure. The scale bars are 2 μm. Reproduced with permission [61]. Copyright 2021, Royal Society of Chemistry.

process can be divided into two steps: a rapid adsorption of the polymer at the interface, followed by a slow accumulation of the polymer with a randomly coiled orientation near the interface. It was shown that the PAA adsorbed to the interface has the configuration with its carboxylic acid groups pointing towards the water phase to maximize hydrophilic interactions, whereas the backbone lies in the plane of the interface to maximize hydrophobic interactions with the oil phase [64].

The specific arrangement of PAA at the oil-water interface is pH-dependent because a higher pH increases the charge density and results in deprotonation of the carboxylic acid groups of the polyelectrolytes (Figure 4c). At a low pH, the protonated PAA contains few charged groups and thus has minimal repulsion interactions, permitting a dense packing at the interface. At a high pH, the deprotonated PAA has a large number of charged carboxyl groups, thus resulting in significant

repulsive interactions that prevent the formation of an ordered packing at the interface. Consequently, the interfacial tension upon the polymer adsorption decreases between pH 1.5 and 4.0, but rises from pH 4.0 to 4.5 and ultimately reaches a constant value of 44 mN/m at higher pH, which is near the interfacial tension of the pure chloroform—water interface.

Geisel et al. investigated the self-assembly and compressibility of a cross-linked, solvent-swollen polymer, poly (N-isopropylacrylamide-*co*-methacrylic acid) (pNIPAM-*co*-MAA), at the decane—water interface [65]. Figure 4d shows the compression isotherms of pNIPAM-*co*-MAA microgels in the charged and uncharged states at the interface. Upon compression, the interfacial pressure rises steeply as the microgel concentration at the interface increases and the microgels start to interact (Figure 4e). With further compression, the microgels could desorb from the interface to form multilayered or buckling structures (Figure 4e) [61]. Comparing the isotherms of microgels at the charged and uncharged states, it was found that at the same interfacial pressure, the charged microgels had a higher interfacial concentration, *i.e.*, smaller area per mass. It indicates that the charged microgels can be compressed more easily than their uncharged counterparts, which is strikingly different from the microgels in bulk. This is because the charged microgels are more dragged into the water phase with a smaller protrusion into the oil phase, thus facilitating corona overlap during compression. In addition, the dangling polymeric chains of charged microgels are softer, and hence easier to be penetrated [61]. Thus, it is the swelling properties of the microgels in different charge states rather than electrostatic interactions that play a vital role in determining their compressibility at the oil-water interface. This behavior of soft polymers at the oil-water interface is completely different from that of solid particles, where electrostatic interactions between particles play the most important role in determining the film compressibility.

Self-assembly of proteins at the oil-water interface

Self-assembled proteins, such as bovine serum albumin (BSA), β-lactoglobulin, lysozyme, and β-casein, at the oil-water interface form stable viscoelastic films that are important for food and nutrition, cosmetic, and pharmaceutical industries [66—68]. The adsorption and self-assembly of a protein at the oil-water interface depend on its thermodynamic stability, flexibility, amphipathicity, molecular size, and surface charge. Besides these intrinsic properties, the protein concentration, pH, ionic strength of the buffer, and the nature of the interface also have great effects on protein adsorption [69—71]. These effects are commonly evaluated with the pendant drop method [72]. Figure 5a illustrates the effect of pH on the adsorption kinetics of β-lactoglobulin at the dodecane—water interface. It was found that at the isoelectric point (pI), proteins adsorbed to the interface rapidly and resulted in a lower equilibrium interfacial tension and higher interfacial shear viscosity than those at other pH [67]. This is because, at the pI, proteins carry a net zero charge, thus minimizing electrostatic repulsions between the adsorbed protein molecules.

An important aspect of protein assembly at a surface is to understand the variation of its secondary structures, such as protein folding. Self-assembly of proteins at a surface or interface is a multi-step process, which can be divided into three distinct regimes as shown in Figure 5b: (I) diffusion from the bulk to the interface, (II) conformational rearrangement and adsorption onto the interface causing a steep decrease in the interfacial tension, and (III) relaxation of the adsorbed layer to increase the monolayer coverage and possible formation of multilayers [66,67,73]. Depending on the structure of the protein and its concentration, this process could take minutes to days before an equilibrium can be reached, mostly due to the protein's conformational variations and protein—protein interactions [66]. Using synchrotron radiation circular dichroism and neutron reflection, it has been found that the secondary structures of BSA, including α-helix, β-sheet, and particularly the random-coil structure, were drastically changed upon adsorption to the hexadecane—water interface [74,75]. These structural changes could facilitate interfacial packing, thus allowing for more protein adsorption especially when its bulk phase concentration increases.

To scrutinize the mechanism underlying these structural changes, tremendous studies have been conducted at the molecular level. A protein molecule possesses hydrophobic or amphiphilic moieties, depending on the three-dimensional folding of the polypeptide chain composed of hydrophilic and hydrophobic amino acids. Increasing hydrophobicity promotes faster adsorption, a greater reduction in interfacial tension, and thus improved emulsifying capabilities. In general, hydrophobic amino acids are hidden in the proteins' interior region in the aqueous phase. However, when the proteins adsorb to an interface, these hydrophobic units form new bonds to interact with adjacent molecules and subsequently result in irreversible protein denaturation and formation of closely-packed, cross-linked and gel-like structures at the interface [67]. Bromley et al. used a wild-type BslA protein and a targeted mutation in the cap domain (L77K) by replacing a hydrophobic leucine with a positively charged, hydrophilic lysine, to determine the mechanism responsible for its adsorption from the aqueous phase to the oil-water interface [76]. In its wild-type form, BslA is a surface-active protein with a hydrophobic cap and a hydrophilic tail while the central hydrophobic residues of the cap are essential for

Figure 5

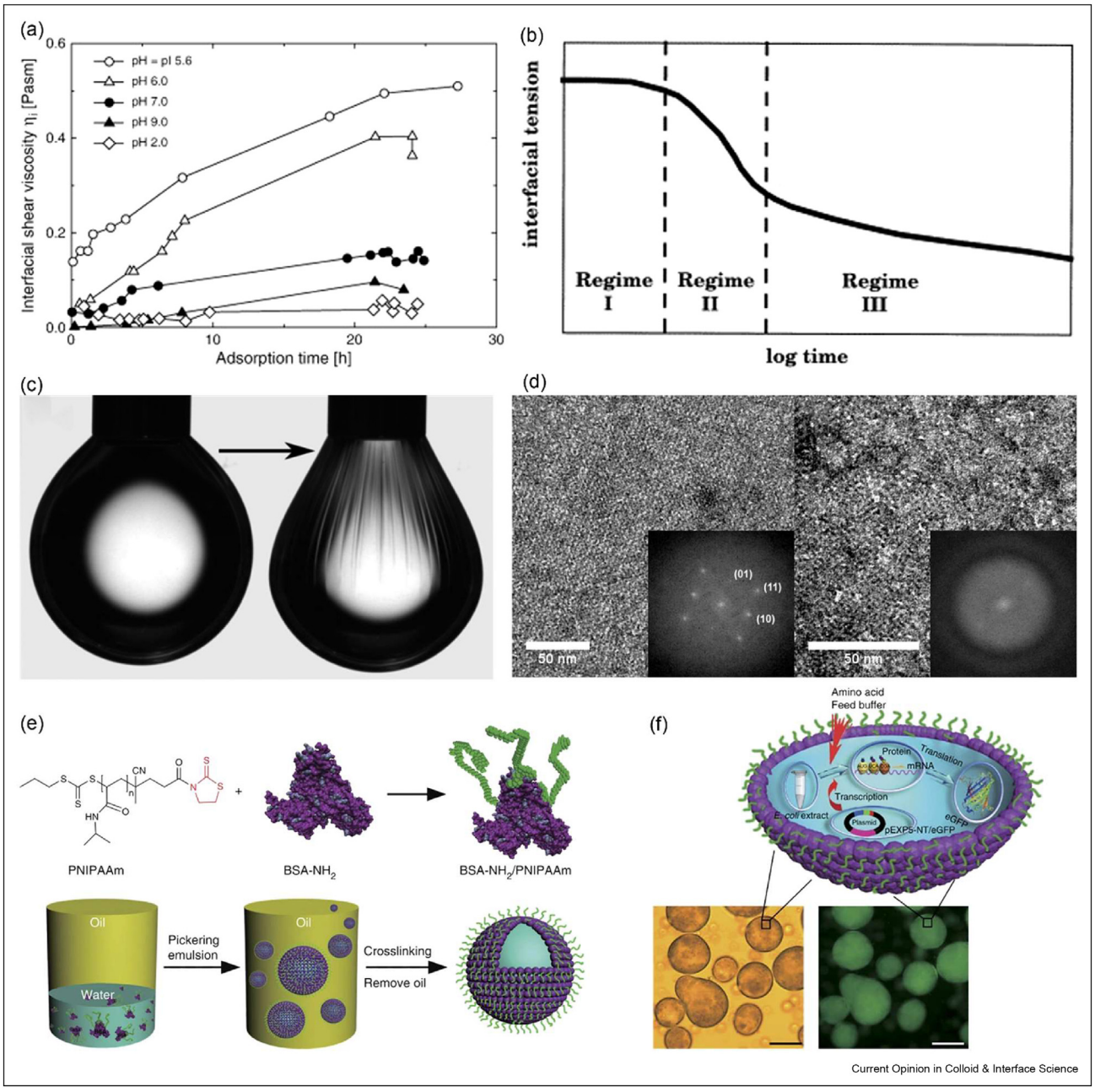

Self-assembly of proteins at the oil-water interface. (**a**) Effect of pH on the interfacial shear viscosity of adsorbed β-lactoglobulin films at the dodecane–water interface as a function of the adsorption time. Reproduced with permission [67]. Copyright 2014, Elsevier. (**b**) Typical adsorption kinetics of a dilute protein solution to the oil-water interface. Reproduced with permission [66]. Copyright 1999, Elsevier. (**c**) A 40-μL droplet of wild-type BslA in glyceryl trioctanoate before and after compression. (**d**) TEM images of the wild-type BslA (left) and BslA-L77K stained with uranyl acetate. Insets show the fast Fourier transforms of the entire TEM images. Reproduced with permission [76]. Copyright 2015, National Academy of Science. (**e**) General procedures for preparing proteinosomes. (**f**) Schematic illustration showing the procedure for cell-free gene expression of enhanced green fluorescent protein in proteinosomes. Reproduced with permission [79]. Copyright 2013, Springer Nature.

the surface activity of this protein. In the aqueous solution, the hydrophobic cap is stabilized by burying the hydrophobic side chains in a random coil conformation [77]. In comparison, the cap residues refold at the interface, with the hydrophobic side chains inserting into the oil phase to generate a three-stranded β-sheet, thus being self-assembled into a well-ordered two-dimensional rectangular lattice that stabilizes the

interface. This can be evidenced by the appearance of persistent wrinkles at the surface of the protein solution droplet in the oil phase (Figure 5c). However, introducing the hydrophilic lysine disrupts the conformation in the aqueous solution so that not all of the hydrophobic groups pack optimally, and their partial exposure facilitates interactions with the interface, thus eliminating the barrier for adsorption ($\sim 10\ k_BT$). Therefore, the adsorption rate of BslA-L77K is dramatically greater than that of the wild-type BslA. TEM images show that after adsorption, the wild-type BslA forms a highly-ordered two-dimensional rectangular lattice enriched in the β-sheets, while the BslA-L77K has a predominantly disorganized arrangement, even though it undergoes a similar random-coil to β-sheet transition (Figure 5d). Owing to the high free energy of adsorption and the formation of the stable lattice structure, the wild-type BslA adsorbs to the oil-water interface irreversibly, while the modified BslA adsorbs reversibly.

Self-assembly of proteins at the oil-water interface has recently found many applications in biomimetics and catalysis [78,79]. Due to their biofunctionality, biodegradability, and bioselectivity, proteins show a great potential as a building block for modeling complex biological systems. Huang et al. reported the self-assembly of BSA-NH_2 at the oil-water interface with the aid of poly (N-isopropylacrylamide) (pNIPAM) for the construction of compartmentalized microarchitectures called proteinosomes (Figure 5e) [79]. This approach is versatile and proteinosomes based on myoglobin-NH_2/pNIPAM or haemoglobin-NH_2/pNIPAM could also be prepared. The shell of these proteinosomes consists of a flexible, structurally robust ultra-thin membrane with a thickness of $\sim$10 nm. These microcompartments show a range of biomimetic properties, including guest-molecule encapsulation, selective permeability, protein synthesis *via* gene expression, and membrane-gated internalized enzyme catalysis. Figure 5f shows that the gene-directed expression of the enhanced green fluorescent protein was successfully achieved in BSA-NH_2/pNIPAM proteinosomes dispersed in an oil [79]. In addition to protocell research, self-assembly of proteins in conjugation with inorganic NPs at the oil-water interface has recently become an important tool for the fabrication of functional catalytic systems with impressive regioselectivity and chemoselectivity [78,80].

Self-assembly of lipids at the oil-water interface

Self-assembled phospholipid monolayers are most commonly studied at the air—water surface as a two-dimensional model for studying lipid polymorphism, surface thermodynamics, and biophysics of cell membranes, pulmonary surfactants, and tear films [81—87]. Figure 6a shows the typical phase diagram of a dipalmitoylphosphatidylcholine (DPPC) monolayer at the air—water surface [86]. Upon lateral compression at a constant temperature, the DPPC monolayer undergoes two first-order phase transitions from a dilute gaseous phase to a liquid-expanded (LE) phase, and from the LE phase to a solid-like tilted-condensed (TC) phase, with the phase transition indicated by a plateau region in the compression isotherms [86]. It was further proved that such phase transitions are reversible upon repeated compression and expansion cycles [83], and similar phase transitions at the air—water surface can be also induced by repeated heating and cooling cycles under constant surface pressures [81].

Compared to the extensive studies of phospholipids at the air—water interface, studies of self-assembled phospholipids at the oil-water interface are relatively scarce, although phospholipids are commonly used as natural emulsifiers in pharmaceutical, food, and cosmetic industries [88]. As shown in Figure 6b, phospholipids are able to dampen thermal fluctuations that wrinkle the oil-water interface, by creating an energy barrier to local surface deformation [89]. Increasing lipid concentration at the interface results in a decreased interfacial tension and a higher barrier to induce deformation by thermal fluctuation. The lack of studies for lipid assembly at the oil-water interface can be partially attributed to the difficulty of adapting the classical Langmuir film techniques to the oil-water interface. Consequently, most studies rely on the pendent drop methods, in which phospholipid self-assembly is formed either by molecular adsorption from the oil phase to the oil-water interface (Figure 6c), or by directly spreading phospholipid molecules at the oil-water interface [90].

For adsorbed phospholipid films, a critical aggregation concentration (CAC) of a phospholipid can be determined by analyzing its adsorption isotherms at the oil-water interface (Figure 6d) [91]. The CAC is equivalent to the critical micelle concentration (CMC) obtained for surfactants in aqueous systems. When the concentration of a phospholipid in the bulk phase reaches its CAC, the phospholipid molecules adsorb to the interface with a full coverage, and any increase in the bulk concentration does not result in a further decrease in the interfacial tension.

For spread phospholipid films, it is important to understand how the oil phase affects the lipid assembly. Thoma and Möhwald studied the effect of three hydrocarbons, *i.e.*, bicyclohexane, dodecane (C_{12}), and hexadecane (C_{16}), on the self-assembly of dipalmitoyl phosphatidylethanolamine (DPPE, 16:0/16:0 PE) at the oil-water interface [92]. Notably, DPPE is insoluble in either of these hydrocarbons. As shown in Figure 6e, a first-order phase transition is indicated by a plateau region in the compression isotherm, similar to the compression isotherms at the air—water surface

Figure 6

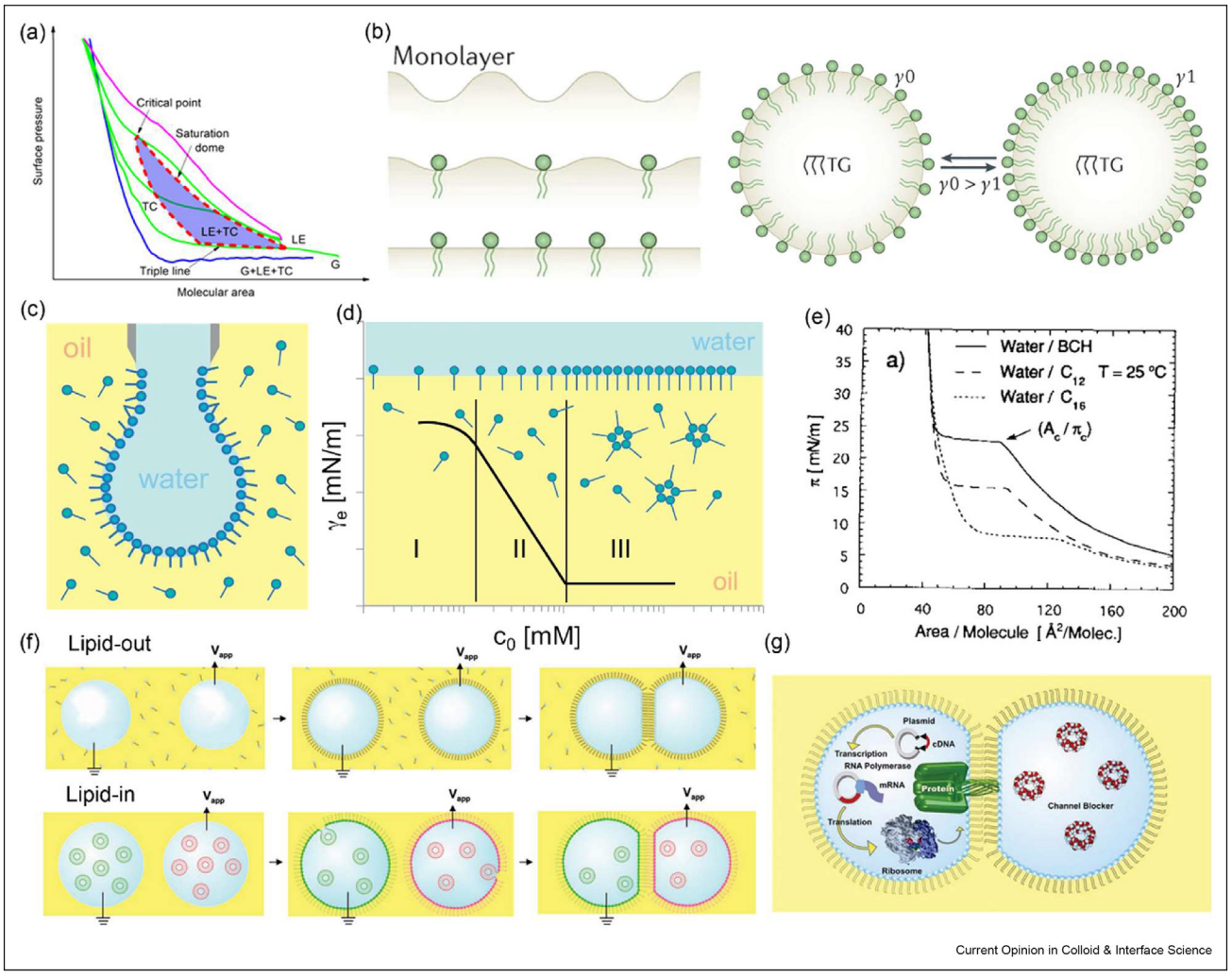

Self-assembly of phospholipids at the oil-water interface. (**a**) A typical phase diagram of phospholipid monolayers at the air–water surface, showing the liquid-expanded (LE) to tilted-condensed (TC) phase transitions at various temperatures. Reproduced with permission [86]. Copyright 2016, American Chemical Society. (**b**) The presence of phospholipids at the oil-water interface can increase the energy barrier for interfacial deformation by thermal fluctuations. Increasing phospholipids at the interface decreases the interfacial tension and increases the emulsion stability. Reproduced with permission [89]. Copyright 2013, Springer Nature. (**c**) Schematic of phospholipid adsorption to the oil-water interface of a pendant drop. (**d**) Typical adsorption isotherms of phospholipids at different concentrations. There are three regimes of lipid solubility: I-molecular dissolved lipids below the CAC; II-lipids adsorb at the interface until full coverage is reached at the CAC; III-lipids start to aggregate at concentrations above the CAC. Reproduced with permission [91]. Copyright 2016, Elsevier. (**e**) Compression isotherms of DPPE at three different oil-water interfaces, *i.e.*, bicyclohexane (BCH)-water, n-dodecane (C_{12})-water, and n-hexadecane (C_{16})-water interfaces, all at the room temperature. Reproduced with permission [92]. Copyright 1994, Elsevier. (**f**) Lipid-out and lipid-in droplet interface bilayers (DIBs) formation. For lipid-out DIBs formation, two aqueous droplets are deposited onto electrodes and submerged in a lipid-containing oil phase. After a stabilization period to allow the formation of lipid monolayers at the oil-water interface, the droplets are brought into contact to form a symmetric bilayer. For lipid-in DIBs formation, two aqueous droplets that contain lipid vesicles of different compositions are deposited into an oil phase. The droplets are brought together to form an axisymmetric bilayer. Reproduced with permission from Ref. [95]. Copyright 2008, American Chemical Society. (**g**) Schematic representation of *in vitro* transcription and translation to form α-hemolysin inside aqueous droplets used to form a DIB. The left-hand droplet contains all of the components necessary for transcription and translation while the right-hand droplet contains a reversible molecular blocker of the α-hemolysin pore. The DIBs can be used as an efficient tool for rapid screening of blockers against the ion channel. Reproduced with permission from Ref. [97]. Copyright 2008, American Chemical Society.

(Figure 6a). The oil phase has shown a significant effect on the surface pressure at which the phase transition occurs, with the highest and lowest phase transition surface pressures for the bicyclohexane–water interface and the hexadecane–water interface, respectively. These results indicate that hexadecane facilities phase transitions in the DPPE monolayer at the oil-water interface, which might be explained by the agreement

of the alkyl chain length between DPPE and hexadecane.

Besides studies of lipid monolayers self-assembled at the oil-water interface, lipid bilayers formed at the interface of two approaching droplets have attracted considerable attention due to their important biological applications. Droplet interface bilayers (DIBs) are stable artificial lipid bilayers formed at the oil-water interface when two phospholipid monolayer-coated aqueous droplets submerged in an oil phase are brought into contact [93,94]. Two distinct techniques have been developed for the fabrication of DIBs, *i.e.*, the lipid-out technique with lipids dissolved in the external oil phase, and the lipid-in technique with lipid vesicles dispersed in the internal aqueous phase (Figure 6f) [95]. The latter is ideal for fabricating asymmetric bilayers since different lipids can be enclosed in the two aqueous droplets. DIBs provide a practical platform for inserting membrane proteins, *e.g.*, ion channels, into artificial cell membranes [96]. Figure 6g shows the incorporation of an ion channel that is synthesized by *in vitro* transcription and translation inside the aqueous droplet [97]. Electrodes inserted into the droplets facilitate precise control of droplets' positions and the measurement of ionic current flowing through embedded ion channels, in order to monitor the electrophysiological characteristics of the ion channels. Thus, DIBs have been engineered to become an efficient chip-based tool for high-throughput single-channel screening. DIBs have also demonstrated potential applications in biosensing, and synthetic cell-mimicking systems for studying the behavior of protein transporters and the prediction of *in vivo* drug transportation [93,98].

Conclusions

We have summarized the colloidal and molecular self-assembly of common materials at the oil-water interface, including particles, polymers, proteins, and lipids. The self-assembly process can be engineered by controlling pH and ionic strength or using external stimuli. Self-assembly at the oil-water interface holds great promise for developing well-structured complex materials useful for many research and industrial applications, such as nanoparticle surfactants, structured liquids, and proteinosomes.

Declaration of competing interest

The authors declare that they have no known competing financial interests or personal relationships that could have appeared to influence the work reported in this paper.

Acknowledgements

This research was supported by the National Science Foundation Grant No. CBET-2011317 (Y.Y.Z.).

References

Papers of particular interest, published within the period of review, have been highlighted as:

* of special interest
** of outstanding interest

1. Yan X, Zhu P, Li J: **Self-assembly and application of diphenylalanine-based nanostructures**. *Chem Soc Rev* 2010, **39**:1877–1890.
2. Jia Y, Li J: **Molecular assembly of rotary and linear motor proteins**. *Acc Chem Res* 2019, **52**:1623–1631.
3. MacFarlane LR, Shaikh H, Garcia-Hernandez JD, Vespa M, Fukui T, Manners I: **Functional nanoparticles through π-conjugated polymer self-assembly**. *Nat Rev Mater* 2021, **6**:7–26.
4. Boles MA, Engel M, Talapin DV: **Self-assembly of colloidal nanocrystals: from intricate structures to functional materials**. *Chem Rev* 2016, **116**:11220–11289.
5. Wasielewski MR: **Self-assembly strategies for integrating light harvesting and charge separation in artificial photosynthetic systems**. *Acc Chem Res* 2009, **42**:1910–1921.
6. Vigderman L, Khanal BP, Zubarev ER: **Functional gold nanorods: synthesis, self-assembly, and sensing applications**. *Adv Mater* 2012, **24**:4811–4841.
7. Zhou Y, Huang W, Liu J, Zhu X, Yan D: **Self-assembly of hyperbranched polymers and its biomedical applications**. *Adv Mater* 2010, **22**:4567–4590.
8. Babu SS, Prasanthkumar S, Ajayaghosh A: **Self-assembled gelators for organic electronics**. *Angew Chem Int Ed* 2012, **51**:1766–1776.
9. Bishop KJM, Wilmer CE, Soh S, Grzybowski BA: **Nanoscale forces and their uses in self-assembly**. *Small* 2009, **5**:1600–1630.
10. Ghosh SK, Böker A: **Self-assembly of nanoparticles in 2D and 3D: recent advances and future trends**. *Macromol Chem Phys* 2019, **220**, 1900196.
11. Shi S, Russell TP: **Nanoparticle assembly at liquid–liquid interfaces: from the nanoscale to mesoscale**. *Adv Mater* 2018, **30**, 1800714.
12. Weiss M, Frohnmayer JP, Benk LT, Haller B, Janiesch J-W, Heitkamp T, *et al.*: **Sequential bottom-up assembly of mechanically stabilized synthetic cells by microfluidics**. *Nat Mater* 2018, **17**:89–96.
13. Lee CH, Tiwari B, Zhang D, Yap YK: **Water purification: oil–water separation by nanotechnology and environmental concerns**. *Environ Sci: Nano* 2017, **4**:514–525.
14. Myint PC, Firoozabadi A: **Thin liquid films in improved oil recovery from low-salinity brine**. *Curr Opin Colloid Interface Sci* 2015, **20**:105–114.
15. Jung Y, Marcus RA: **On the theory of organic catalysis "on water."**. *J Am Chem Soc* 2007, **129**:5492–5502.
16. Acosta E: **Bioavailability of nanoparticles in nutrient and nutraceutical delivery**. *Curr Opin Colloid Interface Sci* 2009, **14**:3–15.
17. ** Cui M, Emrick T, Russell TP: **Stabilizing liquid drops in nonequilibrium shapes by the interfacial jamming of nanoparticles**. *Science* 2013, **342**:460–463.
This is the first study of using electrostatic interactions between charged nanoparticles and polymer ligands to produce nanoparticle surfactants for the construction of nonequilibrium structured liquids.
18. Lawrence MJ, Rees GD: **Microemulsion-based media as novel drug delivery systems**. *Adv Drug Deliv Rev* 2000, **45**:89–121.
19. McClements DJ: **Nanoemulsions versus microemulsions: terminology, differences, and similarities**. *Soft Matter* 2012, **8**:1719–1729.

20. Fink JK: **Chapter 6 - emulsifiers**. In *Hydraulic fracturing chemicals and fluids technology*. Edited by Fink JK, Gulf Professional Publishing; 2013:81–88.

21. Rodríguez-León E, Íñiguez-Palomares R, Urrutia-Bañuelos E, Herrera-Urbina R, Tánori J, Maldonado A: **Self-alignment of silver nanoparticles in highly ordered 2D arrays**. *Nanoscale Res Lett* 2015, **10**:101.

22. Popovetskiy PS, Kolodin AN, Maximovskiy EA, Plyusnin PE, Korolkov IV, Gerasimov EY: **Electrophoretic concentration and production of conductive coatings from silver nanoparticles stabilized with non-ionic surfactant Span 80**. *Colloids Surf A Physicochem Eng Asp* 2021, **625**, 126961.

23. Fortes Martín R, Thünemann AF, Stockmann JM, Radnik J, Koetz J: **From nanoparticle heteroclusters to filament networks by self-assembly at the water–oil interface of reverse microemulsions**. *Langmuir* 2021, **37**:8876–8885.

24. Fortes Martín R, Prietzel C, Koetz J: **Template-mediated self-assembly of magnetite-gold nanoparticle superstructures at the water-oil interface of AOT reverse microemulsions**. *J Colloid Interface Sci* 2021, **581**:44–55.

25. * Dinsmore AD, Hsu MF, Nikolaides MG, Marquez M, Bausch AR, Weitz DA: **Colloidosomes: selectively permeable capsules composed of colloidal particles**. *Science* 2002, **298**:1006–1009.
This is the first study of using self-assembled microparticles at the oil-water interface to produce colloidosomes.

26. Wang X, Liu X, Huang X: **Bioinspired protein-based assembling: toward advanced life-like behaviors**. *Adv Mater* 2020, **32**, 2001436.

27. Park BJ, Brugarolas T, Lee D: **Janus particles at an oil–water interface**. *Soft Matter* 2011, **7**:6413–6417.

28. Binks BP: **Particles as surfactants—similarities and differences**. *Curr Opin Colloid Interface Sci* 2002, **7**:21–41.

29. Jiang H, Sheng Y, Ngai T: **Pickering emulsions: versatility of colloidal particles and recent applications**. *Curr Opin Colloid Interface Sci* 2020, **49**:1–15.

30. Thompson KL, Williams M, Armes SP: **Colloidosomes: synthesis, properties and applications**. *J Colloid Interface Sci* 2015, **447**:217–228.

31. Bago Rodriguez AM, Binks BP: **Capsules from Pickering emulsion templates**. *Curr Opin Colloid Interface Sci* 2019, **44**:107–129.

32. Yang Z, Altantzis T, Zanaga D, Bals S, Tendeloo GV, Pileni M-P: **Supracrystalline colloidal eggs: epitaxial growth and freestanding three-dimensional supracrystals in nanoscaled colloidosomes**. *J Am Chem Soc* 2016, **138**:3493–3500.

33. Stammitti-Scarpone A, Acosta EJ: **Solid-liquid-liquid wettability and its prediction with surface free energy models**. *Adv Colloid Interface Sci* 2019, **264**:28–46.

34. Schrader ME: **Young-dupre revisited**. *Langmuir* 1995, **11**:3585–3589.

35. * Lin Y, Skaff H, Emrick T, Dinsmore AD, Russell TP: **Nanoparticle assembly and transport at liquid-liquid interfaces**. *Science* 2003, **299**:226–229.
This is the first direct observation of particle-size-dependent self-assembly at the oil-water interface.

36. ** Reincke F, Hickey SG, Kegel WK, Vanmaekelbergh D: **Spontaneous assembly of a monolayer of charged gold nanocrystals at the water/oil interface**. *Angew Chem Int Ed* 2004, **43**:458–462.
This is an easy and versatile method to reduce the interfacial energy and to increase adsorption of hydrophilic nanoparticles at the oil-water interface.

37. Duan H, Wang D, Kurth DG, Möhwald H: **Directing self-assembly of nanoparticles at water/oil interfaces**. *Angew Chem Int Ed* 2004, **43**:5639–5642.

38. Booth SG, Dryfe RAW: **Assembly of nanoscale objects at the liquid/liquid interface**. *J Phys Chem C* 2015, **119**:23295–23309.

39. Wang J, Wang D, Sobal NS, Giersig M, Jiang M, Möhwald H: **Stepwise directing of nanocrystals to self-assemble at water/oil interfaces**. *Angew Chem Int Ed* 2006, **45**:7963–7966.

40. Park Y-K, Yoo S-H, Park S: **Assembly of highly ordered nanoparticle monolayers at a water/hexane interface**. *Langmuir* 2007, **23**:10505–10510.

41. Luo ZY, Bai BF: **Retardation of droplet transport in confined microchannel by interfacial jamming of nanoparticles**. *Phys Fluids* 2020, **32**, 087110.

42. Qi J, Yu ZL, Liao GP, Luo ZY, Bai BF: **Effect of nanoparticle surfactants on droplet formation in a flow-focusing microchannel**. *Phys Fluids* 2021, **33**, 112008.

43. Liu X, Kent N, Ceballos A, Streubel R, Jiang Y, Chai Y, *et al.*: **Reconfigurable ferromagnetic liquid droplets**. *Science* 2019, **365**:264–267.

44. Stratford K, Adhikari R, Pagonabarraga I, Desplat J-C, Cates ME: **Colloidal jamming at interfaces: a route to fluid-bicontinuous gels**. *Science* 2005, **309**:2198–2201.

45. Huang C, Sun Z, Cui M, Liu F, Helms BA, Russell TP: **Structured liquids with pH-triggered reconfigurability**. *Adv Mater* 2016, **28**:6612–6618.

46. Chai Y, Lukito A, Jiang Y, Ashby PD, Russell TP: **Fine-tuning nanoparticle packing at water–oil interfaces using ionic strength**. *Nano Lett* 2017, **17**:6453–6457.

47. Feng T, Hoagland DA, Russell TP: **Assembly of acid-functionalized single-walled carbon nanotubes at oil/water interfaces**. *Langmuir* 2014, **30**:1072–1079.

48. Sun S, Xie C, Chen J, Yang Y, Li H, Russell TP, *et al.*: **Responsive interfacial assemblies based on charge-transfer interactions**. *Angew Chem Int Ed* 2021, **60**:26363–26367.

49. ** Sun H, Li L, Russell TP, Shi S: **Photoresponsive structured liquids enabled by molecular recognition at liquid–liquid interfaces**. *J Am Chem Soc* 2020, **142**:8591–8595.
The authors proposed a new type of nanoparticle surfactant based on host-guest molecular recognition at the oil-water interface.

50. Guo X-S, Zhang Z-K, Zhang T-Y, Tong Z-Z, Xu J-T, Fan Z-Q: **Interfacial self-assembly of amphiphilic conjugated block copolymer into 2D nanotapes**. *Soft Matter* 2019, **15**:8790–8799.

51. Chowdhury AU, Taylor GJ, Bocharova V, Sacci RL, Luo Y, McClintic WT, *et al.*: **Insight into the mechanisms driving the self-assembly of functional interfaces: moving from lipids to charged amphiphilic oligomers**. *J Am Chem Soc* 2020, **142**:290–299.

52. Lin L, Chowdhury AU, Ma Y-Z, Sacci RL, Katsaras J, Hong K, *et al.*: **Ion pairing and molecular orientation at liquid/liquid interfaces: self-assembly and function**. *J Phys Chem B* 2022, **126**:2316–2323.

53. Liu Z, Lin L, Li T, Kinnun J, Hong K, Ma Y-Z, *et al.*: **Squeezing out interfacial solvation: the role of hydrogen-bonding in the structural and orientational freedom of molecular self-assembly**. *J Phys Chem Lett* 2022, **13**:2273–2280.

54. Xu R, Liu T, Sun H, Wang B, Shi S, Russell TP: **Interfacial assembly and jamming of polyelectrolyte surfactants: a simple route to print liquids in low-viscosity solution**. *ACS Appl Mater Interfaces* 2020, **12**:18116–18122.

55. Zheng Y, Yu Z, Parker RM, Wu Y, Abell C, Scherman OA: **Interfacial assembly of dendritic microcapsules with host–guest chemistry**. *Nat Commun* 2014, **5**:5772.

56. Balasubramanian V, Herranz-Blanco B, Almeida PV, Hirvonen J, Santos HA: **Multifaceted polymersome platforms: spanning from self-assembly to drug delivery and protocells**. *Prog Polym Sci* 2016, **60**:51–85.

57. Li J-J, Zhou Y-N, Luo Z-H: **Polymeric materials with switchable superwettability for controllable oil/water separation: a comprehensive review**. *Prog Polym Sci* 2018, **87**:1–33.

58. Trantidou T, Friddin M, Elani Y, Brooks NJ, Law RV, Seddon JM, *et al.*: **Engineering compartmentalized biomimetic micro- and nanocontainers**. *ACS Nano* 2017, **11**:6549–6565.

59. Siemes E, Nevskyi O, Sysoiev D, Turnhoff SK, Oppermann A, Huhn T, *et al.*: **Nanoscopic visualization of cross-linking density in polymer networks with diarylethene photoswitches**. *Angew Chem Int Ed* 2018, **57**:12280–12284.

60. Scotti A, Bochenek S, Brugnoni M, Fernandez-Rodriguez MA, Schulte MF, Houston JE, *et al.*: **Exploring the colloid-to-polymer transition for ultra-low crosslinked microgels from three to two dimensions**. *Nat Commun* 2019, **10**:1418.

61. * Bochenek S, Scotti A, Richtering W: **Temperature-sensitive soft microgels at interfaces: air–water versus oil–water**. *Soft Matter* 2021, **17**:976–988.
The authors observed conformational changes of polymer microgels adsorbed to the oil-water interface, different from adsorption to the air–water surface.

62. Schmidt MM, Bochenek S, Gavrilov AA, Potemkin II , Richtering W: **Influence of charges on the behavior of polyelectrolyte microgels confined to oil–water interfaces**. *Langmuir* 2020, **36**:11079–11093.

63. ** Beaman DK, Robertson EJ, Richmond GL: **Ordered polyelectrolyte assembly at the oil-water interface**. *Proc Nation Acad Sci USA* 2012, **109**:3226–3231.
This is a systematic study about the adsorption of polyelectrolytes, and their corresponding interfacial structures at the oil-water interface.

64. Beaman DK, Robertson EJ, Richmond GL: **Unique assembly of charged polymers at the Oil–Water interface**. *Langmuir* 2011, **27**:2104–2106.

65. Geisel K, Isa L, Richtering W: **The compressibility of pH-sensitive microgels at the oil–water interface: higher charge leads to less repulsion**. *Angew Chem Int Ed* 2014, **53**:4905–4909.

66. Beverung CJ, Radke CJ, Blanch HW: **Protein adsorption at the oil/water interface: characterization of adsorption kinetics by dynamic interfacial tension measurements**. *Biophys Chem* 1999, **81**:59–80.

67. Mitropoulos V, Mütze A, Fischer P: **Mechanical properties of protein adsorption layers at the air/water and oil/water interface: a comparison in light of the thermodynamical stability of proteins**. *Adv Colloid Interface Sci* 2014, **206**:195–206.

68. Livney YD: **Milk proteins as vehicles for bioactives**. *Curr Opin Colloid Interface Sci* 2010, **15**:73–83.

69. Fang Y, Dalgleish DG: **Conformation of β-lactoglobulin studied by FTIR: effect of pH, temperature, and adsorption to the oil–water interface**. *J Colloid Interface Sci* 1997, **196**:292–298.

70. Zhang X, Qi B, Xie F, Hu M, Sun Y, Han L, *et al.*: **Emulsion stability and dilatational rheological properties of soy/whey protein isolate complexes at the oil-water interface: influence of pH**. *Food Hydrocolloids* 2021, **113**, 106391.

71. Bergfreund J, Bertsch P, Kuster S, Fischer P: **Effect of oil hydrophobicity on the adsorption and rheology of β-lactoglobulin at oil–water interfaces**. *Langmuir* 2018, **34**:4929–4936.

72. Yang J, Yu K, Zuo YY: **Accuracy of axisymmetric drop shape analysis in determining surface and interfacial tensions**. *Langmuir* 2017, **33**:8914–8923.

73. Yang J, Yu K, Tsuji T, Jha R, Zuo YY: **Determining the surface dilational rheology of surfactant and protein films with a droplet waveform generator**. *J Colloid Interface Sci* 2019, **537**:547–553.

74. Day L, Zhai J, Xu M, Jones NC, Hoffmann SV, Wooster TJ: **Conformational changes of globular proteins adsorbed at oil-in-water emulsion interfaces examined by Synchrotron Radiation Circular Dichroism**. *Food Hydrocolloids* 2014, **34**:78–87.

75. Campana M, Hosking SL, Petkov JT, Tucker IM, Webster JRP, Zarbakhsh A, *et al.*: **Adsorption of bovine serum albumin (BSA) at the oil/water interface: a neutron reflection study**. *Langmuir* 2015, **31**:5614–5622.

76. ** Bromley KM, Morris RJ, Hobley L, Brandani G, Gillespie RMC, McCluskey M, *et al.*: **Interfacial self-assembly of a bacterial hydrophobin**. *Proc Natl Acad Sci USA* 2015, **112**:5419–5424.
This is the first detailed study about the mechanism responsible for protein adsorption to the oil-water interface by comparing the adsorption behaviors of the wild-type protein and its targeted-mutated counterparts.

77. Hobley L, Ostrowski A, Rao FV, Bromley KM, Porter M, Prescott AR, *et al.*: **BslA is a self-assembling bacterial hydrophobin that coats the Bacillus subtilis biofilm**. *Proc Nation Acad Sci USA* 2013, **110**:13600–13605.

78. Samanta B, Yang X-C, Ofir Y, Park M-H, Patra D, Agasti SS, *et al.*: **Catalytic microcapsules assembled from enzyme–nanoparticle conjugates at oil–water interfaces**. *Angew Chem Int Ed* 2009, **48**:5341–5344.

79. Huang X, Li M, Green DC, Williams DS, Patil AJ, Mann S: **Interfacial assembly of protein–polymer nano-conjugates into stimulus-responsive biomimetic protocells**. *Nat Commun* 2013, **4**:2239.

80. Xi Y, Liu B, Wang S, Huang X, Jiang H, Yin S, *et al.*: **Growth of Au nanoparticles on phosphorylated zein protein particles for use as biomimetic catalysts for cascade reactions at the oil–water interface**. *Chem Sci* 2021, **12**:3885–3889.

81. Xu L, Bosiljevac G, Yu K, Zuo YY: **Melting of the dipalmitoylphosphatidylcholine monolayer**. *Langmuir* 2018, **34**:4688–4694.

82. Xu L, Yang Y, Zuo YY: **Atomic force microscopy imaging of adsorbed pulmonary surfactant films**. *Biophys J* 2020, **119**:756–766.

83. Xu L, Zuo YY: **Reversible phase transitions in the phospholipid monolayer**. *Langmuir* 2018, **34**:8694–8700.

84. Xu X, Kang C, Sun R, Zuo YY: **Biophysical properties of tear film lipid layer II. Polymorphism of FAHFA**. *Biophys J* 2022, **121**:451–458.

85. Xu X, Li G, Zuo YY: **Biophysical properties of tear film lipid layer I. Surface tension and surface rheology**. *Biophys J* 2022, **121**:439–450.

86. * Zuo YY, Chen R, Wang X, Yang J, Policova Z, Neumann AW: **Phase transitions in dipalmitoylphosphatidylcholine monolayers**. *Langmuir* 2016, **32**:8501–8506.
This is a comprehensive study of phospholipid phase transitions at the air–water surface and various temperatures using a novel constrained drop surfactometer.

87. Zuo YY, Veldhuizen RAW, Neumann AW, Petersen NO, Possmayer F: **Current perspectives in pulmonary surfactant — inhibition, enhancement and evaluation**. *Biochim Biophys Acta Biomembr* 2008, **1778**:1947–1977.

88. Ozturk B, McClements DJ: **Progress in natural emulsifiers for utilization in food emulsions**. *Curr Opin Food Sci* 2016, **7**:1–6.

89. Thiam AR, Farese Jr RV, Walther TC: **The biophysics and cell biology of lipid droplets**. *Nat Rev Mol Cell Biol* 2013, **14**:775–786.

90. Li J, Miller R, Möhwald H: **Characterisation of phospholipid layers at liquid interfaces 2. Comparison of isotherms of insoluble and soluble films of phospholipids at different fluid/water interfaces**. *Colloids Surf A Physicochem Eng Asp* 1996, **114**:123–130.

91. Hildebrandt E, Sommerling J-H, Guthausen G, Zick K, Stürmer J, Nirschl H, *et al.*: **Phospholipid adsorption at oil in water versus water in oil interfaces: implications for interfacial densities and bulk solubilities**. *Colloids Surf A Physicochem Eng Asp* 2016, **505**:56–63.

92. Thoma M, Möhwald H: **Phospholipid monolayers at hydrocarbon/water interfaces**. *J Colloid Interface Sci* 1994, **162**:340–349.

93. Bayley H, Cronin B, Heron A, Holden MA, Hwang WL, Syeda R, *et al.*: **Droplet interface bilayers**. *Mol Biosyst* 2008, **4**:1191–1208.

94. Funakoshi K, Suzuki H, Takeuchi S: **Lipid bilayer formation by contacting monolayers in a microfluidic device for membrane protein analysis**. *Anal Chem* 2006, **78**:8169–8174.

95. * Hwang WL, Chen M, Cronin B, Holden MA, Bayley H: **Asymmetric droplet interface bilayers**. *J Am Chem Soc* 2008, **130**: 5878–5879.
This is a comprehensive study of approaches used for fabricating droplet interface bilayers.

96. Sacci RL, Scott HL, Liu Z, Bolmatov D, Doughty B, Katsaras J, *et al.*: **Disentangling memristive and memcapacitive effects in droplet interface bilayers using dynamic impedance spectroscopy**. *Adv Electron Mater* 2022, **8**, 2200121.

97. Syeda R, Holden MA, Hwang WL, Bayley H: **Screening blockers against a potassium channel with a droplet interface bilayer array**. *J Am Chem Soc* 2008, **130**:15543–15548.

98. Stephenson EB, Korner JL, Elvira KS: **Challenges and opportunities in achieving the full potential of droplet interface bilayers**. *Nat Chem* 2022, **14**:862–870.